

COMPARISON OF RELIABILITY OF COPPER, GOLD, SILVER, AND PCC WIREBONDS UNDER SUSTAINED OPERATION AT 200°C

Pradeep Lall & Shantanu Deshpande
 Auburn University
 NSF-CAVE3 Electronics Research Center
 AL, USA
 lall@auburn.edu

Luu Nguyen
 Texas Instruments, Inc.
 CA, USA

ABSTRACT

Semiconductor packaging industry is transitioning to use of alternate lower cost wirebond materials to replace gold (Au) wire which is often used in high-reliability applications. Typical wire diameters vary between 0.8mil to 2mil. Recent increases in the gold-price have motivated the industry to search for alternate materials candidates for use in wirebonding. Three of the leading wirebonding candidates are Silver (Ag), Copper (Cu), and Palladium Coated Copper (PCC). The new material candidates are inexpensive in comparison with gold and may have better electrical, and thermal properties, which is advantageous for fine pitch-high density electronics. The transition, however, comes along with few trade-offs such as narrow process window, higher wire-hardness, increased propensity for chip-cratering, lack of reliability knowledge base of when deployed in harsh environment applications. Relationship between mechanical degradation of the wirebond and the change in electric response needs to be established for better understanding of the failure modes and their respective mechanisms. Understanding the physics of damage progression may provide insights into the process parameters for manufacture of more robust interconnects. In this paper, a detailed study of the electrical and mechanical degradation of wirebonds under high temperature exposure is presented. Four wirebond candidates (Au, Ag, Cu and PCC) bonded onto Aluminum (Al) pad were subjected to high temperature storage life until failure to study the degradation of the bond-wire interface. Same package architecture and electronic molding compound (EMC) were used for all four candidates. Detailed analysis of intermetallic (IMC) phase evolution is presented along with quantification of the phases and their evolution over time. Ball shear strength was measured after decapsulation. Measurements of shear strength, shear failure modes, and IMC composition have been correlated with the change in the electrical response. Change in shear strength and different shear failure modes for different wirebond systems are discussed in the paper.

INTRODUCTION

Wirebonds are widely used first-level interconnects between the semiconductor-chip with the substrate of the package. Adaptability of the wirebonding morphology to a number of package types in addition to the trend towards low-profile formed wires has resulted in their continued use in newer chip-scale form-factor and stacked chip packages. Typical bond wires range in 0.8-2 mil in diameters. Copper wires may be thermosonic or ultrasonic bonded on aluminum pads either on-chip or on-substrate [1]. The intense interest in the viability and manufacturing process development of copper wires has been motivated by search for cost-effective alternatives and the increase in gold prices. Copper, silver and palladium-coated copper are amongst the top-choices for alternative materials. Electrical, thermal and mechanical properties of alternative wirebond candidate materials are shown in Table 1.

Table 1. Material Properties of Cu, Ag, Au [2]

| Property | Unit | Cu | Au | Ag |
|-------------------------------|------------------|---------|--------|---------|
| Thermal Conductivity | W/mK | 400 | 320 | 430 |
| Electrical Resistivity | Ωm | 1.72e-8 | 2.2e-8 | 1.63e-8 |
| Young's Modulus | GPa | 130 | 60 | 82.5 |
| Poisson Ratio | | 0.34 | 0.44 | 0.364 |
| Yield Stress | MPa | 200 | 32.7 | 45.5 |
| CTE | ppm/°C | 16.5 | 14.4 | 18.9 |
| Vickers Hardness | MPa | 369 | 216 | 251 |

Copper wires have higher thermal and electric conductivity in comparison with gold, which enables smaller diameter Cu wires to carry identical current as a gold wire without overheating. Cu wire is mechanically stronger than Au wire, which reduces the propensity for wire sweep during the molding process [3]. Cu-Al IMC has slower growth rate than Au-Al IMC, which makes Cu wires more reliable for applications needing prolonged storage at high temperature

[4], [5]. Temperature dependence of CuAl intermetallic has been studied and the stability of Cu_9Al_4 (Copper rich), CuAl and CuAl_2 (Aluminum rich) reported [6]. Prolonged aging has been found to cause breakdown of the IMC along the periphery of the wirebond. Aging is accompanied with the initiation and propagation of crack towards center of the ball bond followed by complete cracking of the interface. Corrosion of the Cu rich phase, Cu_9Al_4 has been found to dominate the corrosion process [5][6][7][8]. The higher reactivity of copper in comparison with gold necessitates a bigger focus on surrounding materials including electronic molding compounds (EMCs), die attach, and bond pads. Higher chlorine content in EMCs has been shown to cause a significant reduction in copper wirebond time-to-failure. Acidic pH values of EMCs accelerate the corrosion reaction resulting in faster rates of degradation [9][10][11][12]. Copper wires may be coated with palladium (Pd) to increase the adhesion between the wire and the second bond on the substrate [12]. The presence of palladium has also been shown to reduce the diffusion rate of Cu-Al wirebond and prolong the shelf life of the wirebond under HTSL as well as HAST conditions [13][14][15][16]. Microstructural degradation mechanisms of the palladium coated copper wire have yet to be correlated with reliability and onset of degradation under harsh operating conditions.

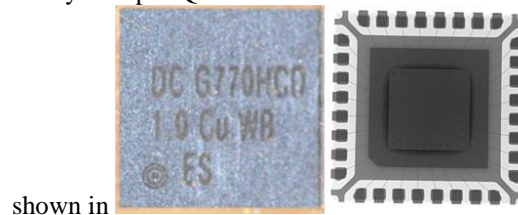
Silver (Ag) wires have higher thermal conductivity and lower electric resistivity in comparison with copper and aluminum, which makes it a good candidate for power electronics. Silver has a higher elastic modulus and hardness than gold, but lower than copper, which makes silver wires easier to bond. Even though bonding Ag on Al pad has wider process window, it is still significantly costlier than Cu and PCC wire bonding [1]. Studies on the bondability [17] of the Ag wires on different pad materials and found excellent ability to form low resistance first-level interconnects to a number of different pad materials. Studies on the bond-interface intermetallics [18] report two types of IMCs formed during high temperature testing of pure silver as well as silver alloy wires. Data on both copper and silver wires has been reported in some of the reliability tests. The corrosion of the silver intermetallic including Ag_3Al and Ag_2Al [19] has been studied in HAST due to attack of ionic contamination in the EMC. In order to build a reliability model and assess damage progression, detailed studies are needed for the initiation and progression of IMC phases, and their correlation with the interface cracks at high ambient temperatures.

Study presented in this paper focuses on the response of different wirebond systems, bonded on the Al pad subjected to high temperature storage life. Packages were molded with EMC candidate designed to sustain temperatures of about 200°C . Electric responses of wirebonds was measured and correlated with the change in morphology of the bond-pad interface. Cu, Au and PCC wirebonds were decapsulated to check evolution in shear strength of wirebond as a function of aging duration. Change in magnitude of shear strength and failure modes were then correlated with IMC growth

and increase in resistance. This will provide better understanding of degradation mechanisms for the wirebond systems and address the reliability concerns.

TEST VEHICLE

Thirty-two pin QFN devices were selected for this study as



shown in

Figure 1. Package attributes are shown in Table 2. Identical packages with Gold (Au), Copper (Cu), and Silver (Ag) wires, 1 mil in diameter, wire bonded onto $1\mu\text{m}$ thick Al pad were fabricated. In addition, packages with 0.8 mil diameter PCC wire were bonded onto $1\mu\text{m}$ thick Aluminum (Al) pad. All the packages were molded with the epoxy-molding compound, specifically designed for high temperature application capable of sustained operation at 200°C . EMC had 5ppm Cl^- ion concentration, pH value of 6 and a glass transition temperature (T_g) of 150°C . Packages were post mold cured at 175°C for 4 hours. In each package, there are thirty-two wirebonds. Two wirebonds were connected to each other to form a pair. Thus, each package has a total of 16-pairs of wirebonds.

Table 2. Package Dimensions

| Parameter | Dimensions (mm) |
|-----------|-----------------|
| Width | 5.02 |
| Length | 5.02 |
| Height | 1.52 |
| Pitch | 0.5 |

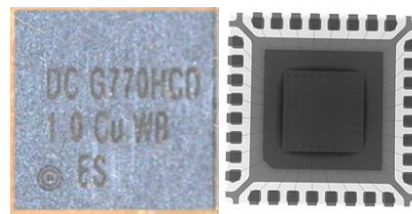


Figure 1. Optical and X-ray image of the Package

TEST MATRIX

All packages were subjected to 200°C isothermal aging in order to simulate sustained high temperature operation. Packages were taken out at periodic time intervals and resistance of the wirebond pairs was measured till failure using high resolution capable resistance spectroscopy technique. A 20-percent degradation in the parts was treated as a failure threshold for the parts. Packages were then cross-sectioned to analyze change in the morphology at bond-pad interface. Chemical etchants were used to enhance contrast between different IMC phases. Composition of IMC phases was confirmed using EDX analysis. Thickness of IMC layer was measured at each observation point.

Measurements of the IMC thickness were made at multiple points, as shown in Figure 2. Average value of all the readings was then considered as the final IMC thickness for the specific test condition. A subset of the packages was then decapsulated using fuming acids and ball shear test was performed on the ball-bond to study change in shear strength of the wirebond interface during HTSL. Ball shear test was performed using DAGE2400 ball shear tester. Shear tool height was set to be 2.5 μ m above aluminum pad. Shear tool speed was 150 μ m/s. Shear failure modes were then analyzed using scanning electron microscopy (SEM). Au-wirebonded packages were decapsulated using pure fuming nitric acid. Cu and PCC Wirebonded packages were decapsulated using chemistry suggested in [20]. Change in electric response of the package was then correlated with the change in morphology of bond wire interface and with the change in shear change along with evolution of shear failure modes.

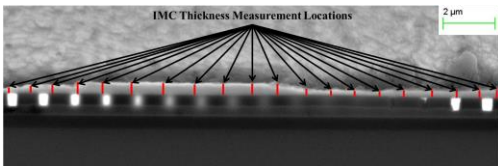


Figure 2. IMC Thickness Measurement

EXPERIMENTAL DATA

Experimental measurements of reliability in high-temperature storage life (HTSL) on four wirebond material systems are discussed in this section. Evolution in the electrical resistance, IMC thickness, and shear strength is presented for each of the material systems.

Cu-Al Wirebond

Figure 3 shows change in resistance of Cu-Al wirebond system under sustained exposure to 200°C ambient temperature. Copper wirebonded package failed after 720 hours of thermal exposure. Red dashed line in Figure 3 shows 20-percent failure threshold for electrical resistance. The wirebond system exhibits a nearly constant initial rate of increase of resistance. The degradation rate showed an increase after initial 5-percent change in resistance. Figure 4 shows the SEM images of the cross-section of bond pad interface. Initially in as bonded state very thin layer of IMC was present. Significant growth in intermetallics was observed between the initial pristine bond and the final failure at 720-hours (Figure 4). IMC thickness was measured at each time interval at several locations in several wirebonds as explained earlier in Figure 2. Growth of the IMCs was accompanied with the diffusion of the aluminum bond pad into the IMC layer and the eventual consumption of the Al pad and bond lift at failure.

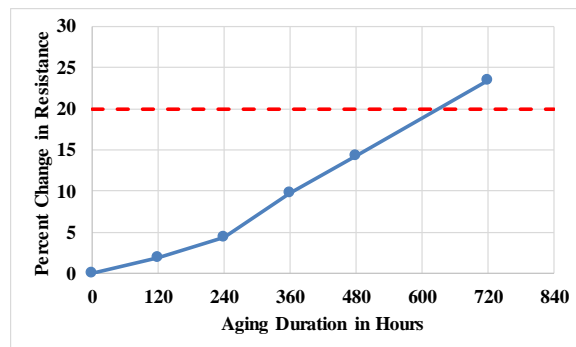


Figure 3. Increase in the resistance of Cu wirebonds at 200°C aging temperature.

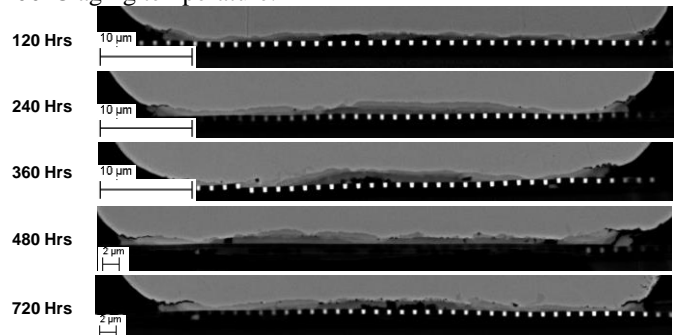


Figure 4. Growth of Cu-Al IMC at bond-pad interface

Figure 5 shows ln-ln plot of an IMC thickness against aging duration. Fit of the experimental data exhibits an exponent value of time of 0.4764. The observed experimental value is close to the theoretical value of 0.5 for Fickian based diffusion. Initial growth rate of IMC is higher in comparison with the latter stages of damage progression. Experimental measurements indicate that the growth rate decreased as the aging duration increased. Different phases of the IMC, which are present between copper and aluminum, have different physical properties and affect the overall diffusion rate. Figure 6 shows that three distinct phases found at the Cu-Al interface. EDX point scans were performed at different locations to identify composition of the phases. Results of the point scan are shown in Table 3. The predominant IMC phase near copper-wire interface (point A) was Cu_9Al_4 , the phase present near Al pad (point C) was CuAl_2 , and the phase in the middle (point B) was CuAl as shown in Table 3. The results are consistent with results published earlier [1][6][7][21].

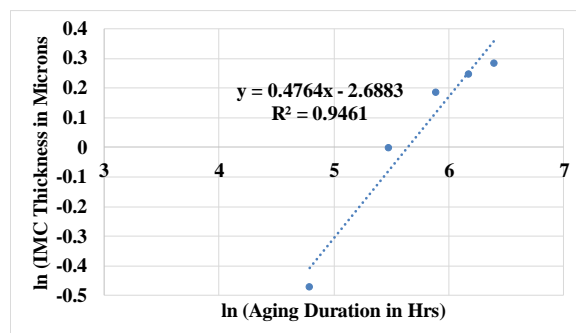


Figure 5. log-log plot of IMC thickness vs aging duration

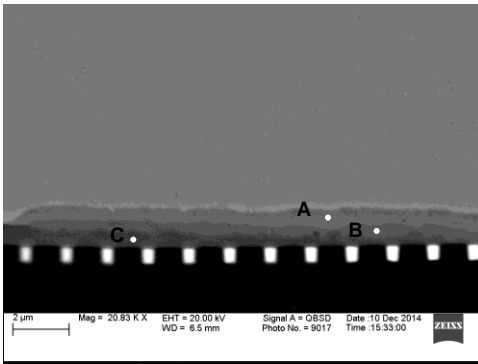


Figure 6. Phases in Cu-Al wirebond system due to exposure to high temperature

Table 3. EDX analysis of IMC phases at point A, B and C.

| Element | Percent Atomic Content | | |
|---------|------------------------|---------|---------|
| | Point A | Point B | Point C |
| Al | 30.96 | 48.64 | 50.63 |
| Cu | 65.48 | 47.91 | 29.18 |
| Au | 3.56 | 3.45 | 1.79 |
| Si | 0.00 | 0.00 | 18.40 |

Figure 7 shows the evolution of various IMC phases during the testing. Only one phase CuAl_2 was present in as-bonded state. However, after 120 hours of aging, all three phases were observed. As the aging duration increases, Cu_9Al_4 phase was found to be dominating and started to consume other two phases. Increase in the thickness of IMC layer dropped significantly because the Al pad was completely consumed at this point (after 240 hours). However, due to abundant supply of the Cu from the wire-side of the bond, and lack of free Al due to the limited thickness of the thin bondpad, thickness of the Cu-rich phase (Cu_9Al_4 ; indicated in green in Figure 7) continued to increase. Subsequent to 720 hours of thermal aging, CuAl layer was barely visible. It is expected that if the part is aged for additional period of time, eventually Cu-rich phase will consume the remaining two IMC phases and convert them into Cu_9Al_4 [1], [6], [21], [22].

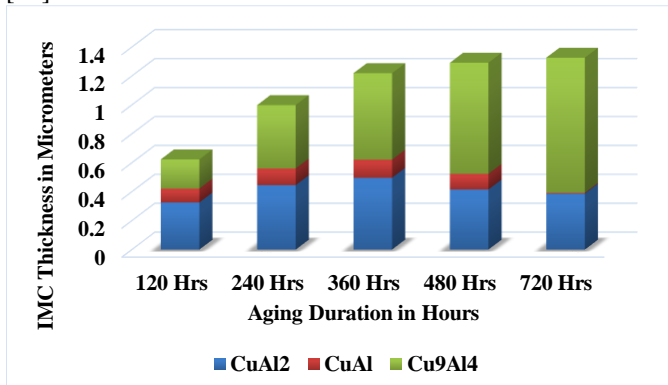


Figure 7. Evolution of different IMC phases due to high temperature exposure in Cu-Al WB

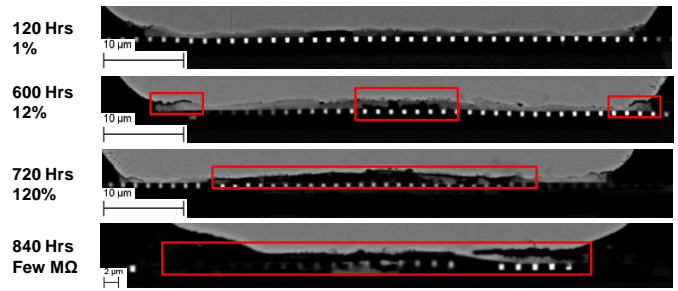


Figure 8. Crack initiation and propagation in Cu-Al WB system

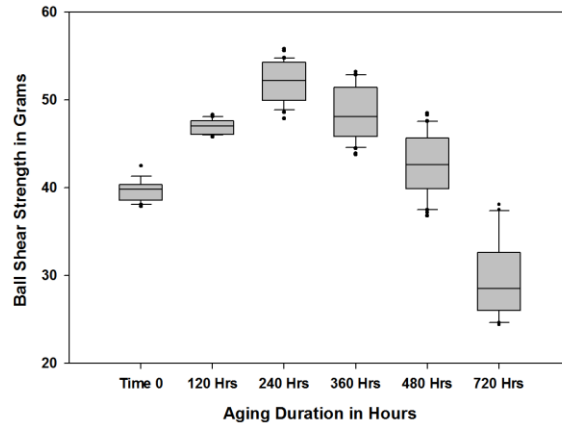


Figure 9. Change in shear strength of bond-pad interface as a function of time for Cu-Al WB.

Figure 8 shows the cracking observed at the wirebond interface. After 120 hours of aging, crack was found along the periphery of the ball bond at the interface of Cu rich IMC phase and Cu. This cracking is due to the corrosion of an IMC. Corrosion process takes place in the presence of an ionic contamination, which is released by degraded molding compound and very high ambient temperature [4], [12], [23]. The crack continued to grow towards the center of the wirebond as the part was subjected to addition duration of high-temperature operation. After 240 hours of aging, due to extremely high temperature and complete consumption of Al pad, silicon oxide which is present below the pad started to diffuse into the ball bond. This effect can be seen predominantly at the center of the ball bond as shown in Figure 8 (600 hours onwards). This defect starts from the center of the ball bond because IMC distribution at the center is uniform and consistent as compared with the edges. Figure 9 shows the change in the shear strength of the wirebonds due to accelerated aging. Each box plot consists of 32 data points. Initial shear strength was in the neighborhood of 40 grams, and it increased to 52 grams after 240 hours of thermal aging. Further aging caused drop in the shear strength and at the time of the failure, with a recorded strength of 30 grams. Drop in the shear strength of the wirebond interconnect indicates weaker connection either due to growth of intermetallics or consumption of the aluminum bond pad. Sheared surfaces were analyzed using SEM to identify different failure modes.

Two modes were identified as shown in Figure 10. Mode I showed little or no residue of Cu or IMC on the sheared surface. Instead, peeling of Al pad was observed. This

failure mode ensures strong mechanical bond between Cu and IMC and is a desirable mode of failure. Mode II on the other hand showed residues of Cu or Cu-Al IMC on the sheared surface, as shown in (B). The residues were concentrated along the periphery of the ball bond. This proves that the link between IMC and Cu ball bond along the periphery was the weakest. A clean crack was observed at the center of the ball bond near the SiO₂ interface, indicating that IMC-Cu interface was still strong, while IMC-silicon oxide interface was the weakest. Complete consumption of the Al pad caused localized detachment at the interface leading to the crack observed in mode II type failure, at the center of the wirebond. The shear failure modes are consistent with the peripheral cracking, and complete consumption of Al pad found during the cross-sectioning (Figure 8). Figure 11 shows an evolution of the shear failure modes as the aging duration increases. During the initial part of aging, till 240 hours, mode I type is dominant. However, after that mode II became dominant and at the time of failure, only mode II was observed.

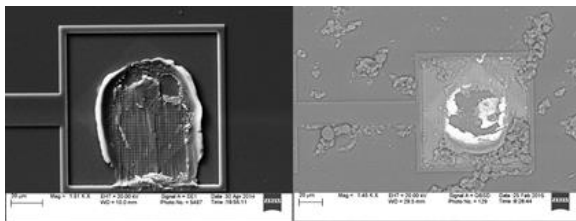


Figure 10. Shear failure modes (A) Mode I (B) Mode II

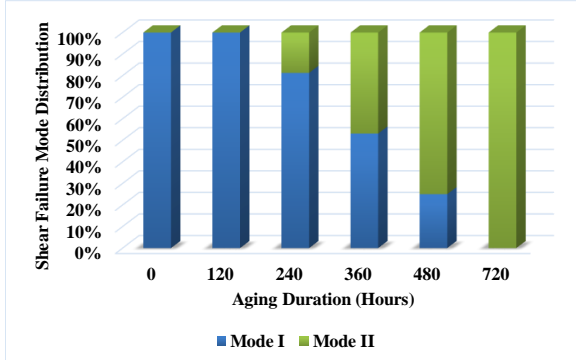


Figure 11. Evolution of shear failure modes in Cu-Al WB

The initial increase in resistance (until 240 hours) takes place at slower rate compared with the later damage progression. This increase in resistance can be attributed to the growth different phases of IMC, which have much higher resistivity than Cu and Al [24]. During the initial stages of IMC growth, the increased diffusion makes the bond stronger, increasing the shear strength of the wirebonds as shown in Figure 9. Mode I type shear failure mode is dominant during this phase, which reflects excellent health of the wirebond. With the increase in aging duration, a rapid increase in the resistance was observed. This can be attributed to the reduction in area available for electron flow due to peripheral crack propagation and localized detachment of IMC and silicon dioxide (Figure 8). The physical detachments and degradation of interface results in

the eventual reduction of shear strength from 52 grams to 30 grams (Figure 9). Mode II type shear failure becomes dominant during the process, which confirms the findings related to Al-pad consumption and its effect on the shear strength of the ball bond.

PCC-Al Wirebond

Figure 12 shows change in the resistance of the PCC wirebond due to aging at high temperature. Red dashed line in the plot shows the 20-percent failure threshold for resistance change. After aging for 800 hours, change in resistance of the wirebonds was more than 20%. Rate of increase in resistance was slow during initial 5% change. After that, the rate increased and package failed at 800-hour interval. Figure 13 shows SEM images of bond-pad interface. Thicker IMC was observed for parts aged for longer duration. Thickness of the IMC was measured at each time interval and log plot of time versus thickness is shown in Figure 14.

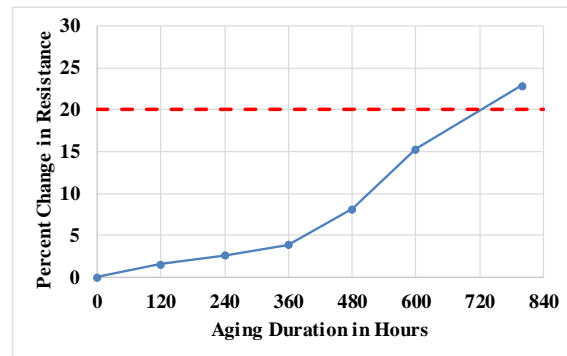


Figure 12. Increase in Resistance of PCC wirebonds at 200°C aging temperature.

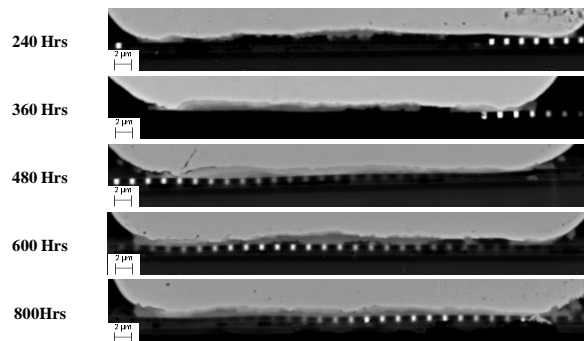


Figure 13. Growth of PCC-Al IMC at bond-pad interface

Maximum thickness of the IMC was 1.20µm. This was lower than the maximum thickness of Cu-Al IMC, which was 1.33µm. Exponent value of time was found to be 0.5018 (Figure 14), which indicates that IMC growth was diffusion driven. Figure 15 shows close-up view of the three different phases found in the IMC layer. EDX point analysis was performed at A, B, and C point. Point A was Cu rich phase (Cu₉Al₄), and point C was Al rich phase (CuAl₂). Point B had equal content of both element (CuAl). Results of the EDX point scan are presented in Table 4.

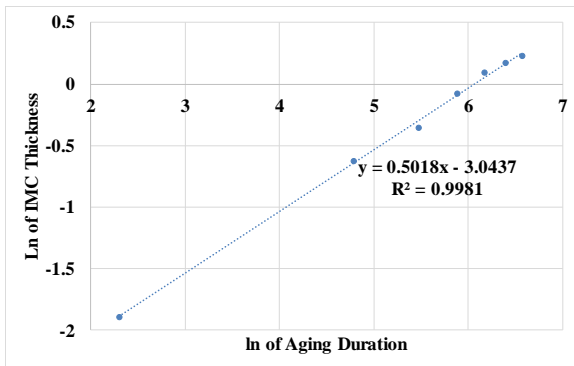


Figure 14. IMC thickness vs aging duration in PCC WB

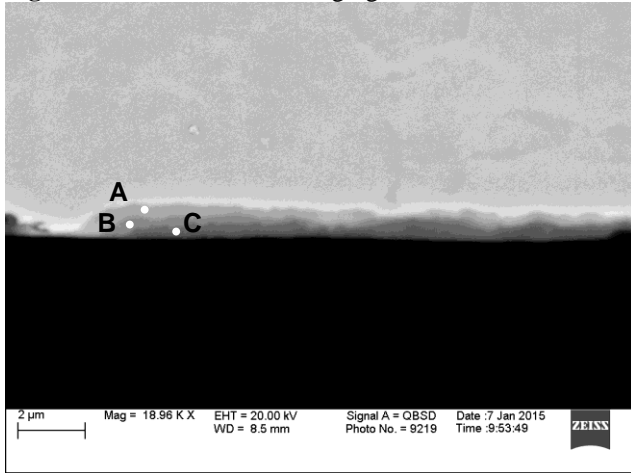


Figure 15. Phases in PCC-Al wirebond system due to exposure to high temperature

Table 4. EDX analysis of IMC phases at point A, B, and C.

| Element | Percent Atomic Content | | |
|---------|------------------------|---------|---------|
| | Point A | Point B | Point C |
| Al | 31.58 | 48.04 | 62.80 |
| Cu | 62.01 | 46.57 | 30.49 |
| Au | 4.28 | 4.48 | 6.71 |
| Pd | 2.13 | 0.91 | 0.00 |

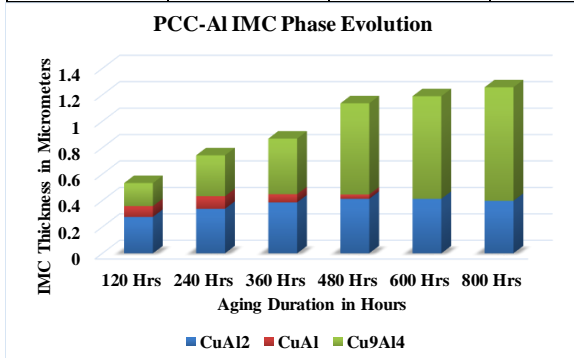


Figure 16. Evolution of different IMC phases due to high temperature exposure

Very small amount of Pd was found in the phases near to Cu ball, while it was absent in Al rich phase. Presence of Pd along the bond-pad interface seemed to act as a diffusion barrier and slowed down the growth of the IMC, making PCC wires slightly more reliable than bare Cu wires [25], [26], [27]. Figure 16 shows evolution of IMC phases

over time. Initially, after 120 hours of aging, three phases of copper-aluminum intermetallics were found. However, after 480 hours of aging, CuAl IMC layer diminishes with the emergence of the copper rich phase (Cu_9Al_4) and simultaneous increase in the thickness of CuAl_2 phase. Continuation of thermal aging results in the reduction in the occurrence of the CuAl_2 phase, and transformation into Cu rich phase. The appearance and growth of the intermetallics is impacted by the abundance of copper in the ball and diffusion process, which have an Arrhenius dependence on temperature.

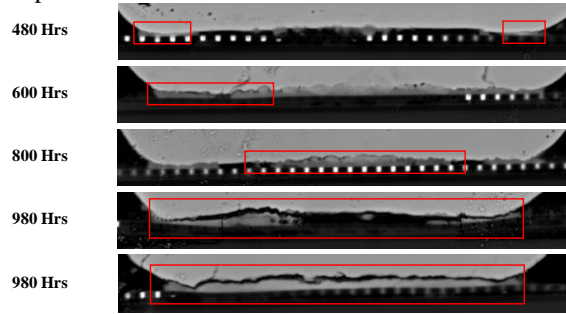


Figure 17. Crack initiation and propagation in PCC-Al WB system

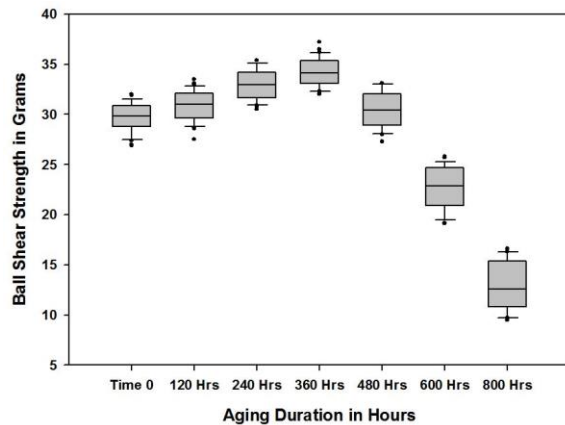


Figure 18. Change in shear strength of bond-pad interface as a function of time.

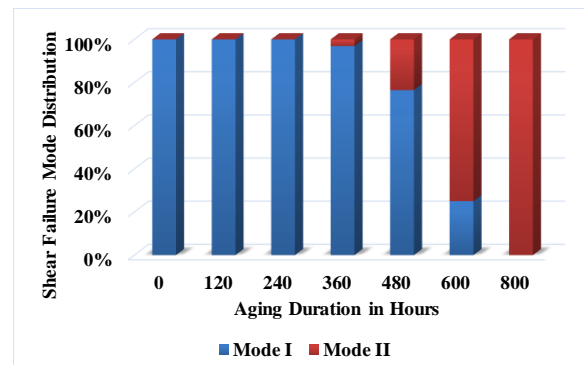


Figure 19. Evolution of shear failure modes

Figure 17 shows crack initiation and propagation at the bond pad interface as a function of time in HTSL for the PCC-Al wirebond system. Corrosion crack originates at the periphery of the ball bond during the initial stages. With the

increase in aging time, the crack propagates towards the center of the ball bond. This peripheral origination and center-progression of cracking is observed in-between Cu rich phase and Cu ball bond. If the part is aged for prolonged period (980 hrs), complete cracking of the interface resulting into detachment of interconnect was observed. Degradation of the PCC and bare Cu wirebond follow similar degradation mechanisms. Presence of Pd in case of PCC wirebond seems to delay the degradation process by small amount. Figure 18 shows evolution of shear strength of the ball bond. Initial values of the ball shear strength were found to be in the neighborhood of 30 grams. The ball shear strength increases till 360 hours of thermal aging. Further aging reduces the shear strength to a value of 12 grams at 800 hours of thermal aging. Sheared surfaces were observed using SEM. Based on the morphology of the remaining area, shear failure modes were divided into two types. Failure modes for bare Cu and PCC were the same. Mode I type failure mode indicates strong bond between PCC and Al, and Mode II type indicates presence of cracking and degraded surface.

Figure 19 shows evolution of the shear failure modes. During first 360 hours of aging, mode I type failure mode was dominant, accompanied by increase in shear strength due to the initial growth of the IMC, which makes bond stronger. Subsequent to achieving the maximum value of shear strength, the IMC starts to degrade and cracks initiates at the periphery of the bond as shown in Figure 17, making the wirebond weaker. Degradation in the shear strength of the bond is accompanied with the dominance of mode II type failures, although mode I failure modes still exist in the distribution of the test population. Subsequent to 800 hours of aging, only mode II type failure was observed at the sheared surface. Decrease in shear strength is also accompanied with the rapid increase in the bond resistance as shown in Figure 12. This rapid growth in resistance could be contributed to the thicker IMC, and the degradation of the IMC which reduces the contact area resulting into higher resistance. Overall distribution of the failure modes for PCC wires was similar to the Cu wires. However, the presence of Pd at the bond pad delayed the degradation.

Ag-Al Wirebond

Figure 20 shows change in resistance of Ag wirebonds subjected to aging at high temperature. Red dashed line in the plot shows the 20-percent failure threshold. Majority of the packages in the Ag test population failed after 840 hours of thermal aging, which is slightly higher in comparison with the time to failure for the PCC wire. Unlike the Cu and PCC wires, Ag wires show approximately linear trend of change in resistance until 720 hours of aging. Figure 21 shows growth of IMC at Ag-Al interface due to high temperature exposure. Even after 120 hours of aging, significant IMC was present at the interface. IMC thickness increases as parts were subjected for aging for longer duration. Ag wirebonds had overall thicker IMC formation and growth than Cu and PCC wires. Log-log plot of IMC thickness and time is shown in Figure 22. Time exponent

for the Ag wirebond was 0.4, which was far from ideal value of 0.5. Even through IMC growth is diffusion driven, it does not follow Fickian diffusion.

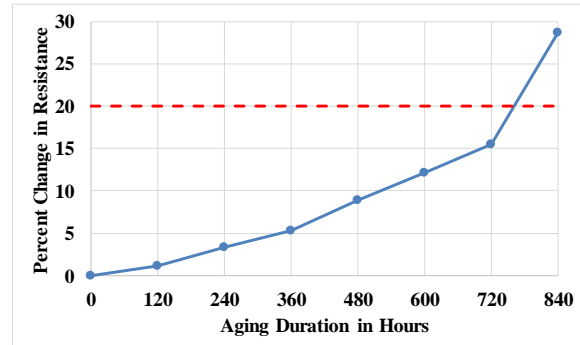


Figure 20. Increase in Resistance of Ag-Al wirebonds at 200°C aging temperature.

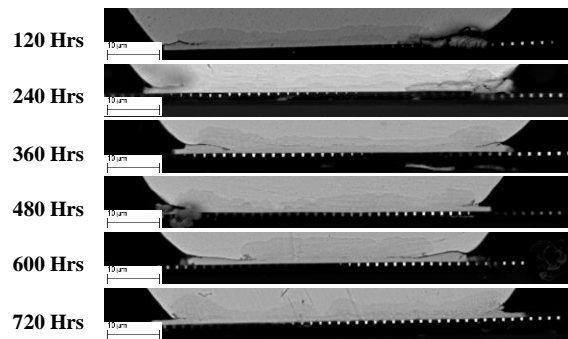


Figure 21. Growth of Ag-Al IMC at bond-pad interface

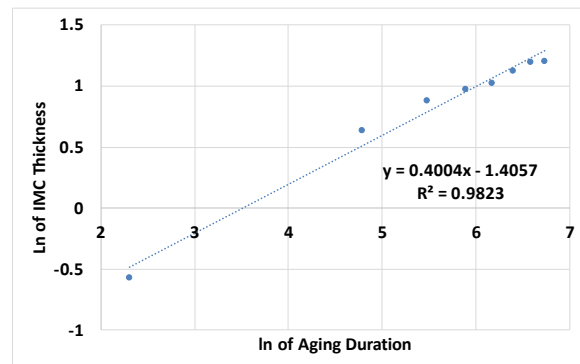


Figure 22. log-log plot of IMC thickness vs aging duration

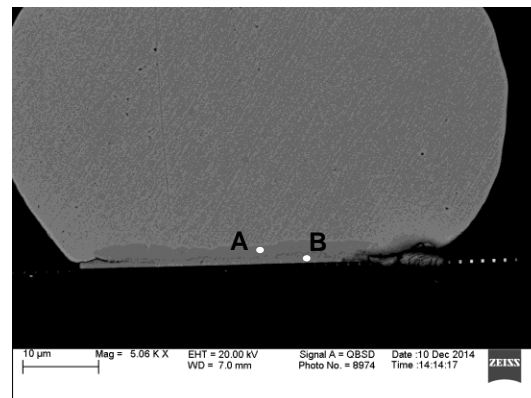


Figure 23. Phases in Ag-Al WB system under exposure to high temperature

Table 5. EDX analysis of IMC phases at point A, B.

| Element | Percent Atomic Content | |
|---------|------------------------|---------|
| | Point A | Point B |
| Al | 25.02 | 33.48 |
| Ag | 73.26 | 64.12 |
| Au | 1.72 | 2.4 |

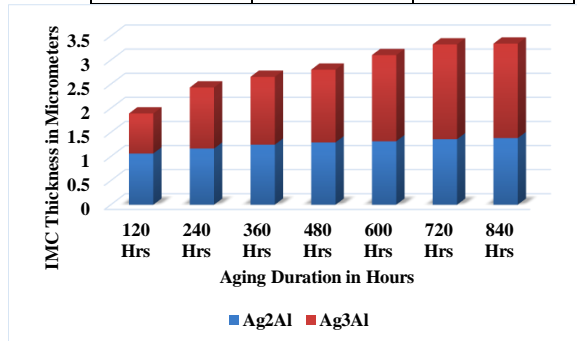


Figure 24. Evolution of different IMC phases due to high temperature exposure

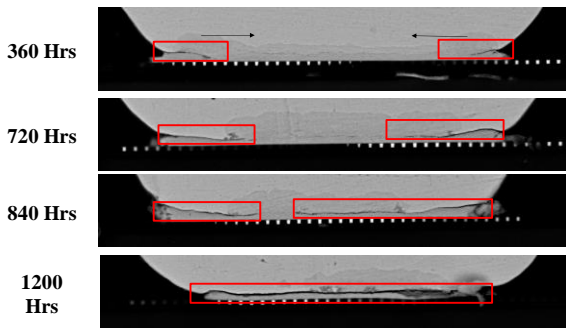


Figure 25. Crack initialization and propagation in Ag-Al WB system

This could be contributed to thicker IMC formation. IMC compounds often have different physical properties than the individual elements from which they are made off. Thicker IMC indicates that Ag or Al had to travel long distance via IMCs to form new compounds. Higher thickness of IMC could affect the rate at which Ag is diffusing in the Al pad and affect IMC growth rate. The Ag-Al bond-pad interface has two different phases of IMCs including a top layer (near ball bond) consisting of Ag₃Al compound, and a bottom layer (near bond pad) consisting of Ag₂Al. EDX point scans were performed at points A and B as shown in Figure 23. Results show that even though both layers were Ag-rich layers, they had different formulations. These measurements were in agreement with results reported in earlier articles [18][19][28][28]. Figure 24 shows evolution of the IMC phases due to high temperature aging. During the initial stage of aging, both phases exhibited growth in thickness. Subsequent to 480 hours of aging, Ag₃Al was found to be rapidly evolving than Ag₂Al. this can be contributed to limited supply of Al from the very thin pad and constant supply of Ag from the ball bond. Further, after 840 hours of

testing, both phases were present, but Ag₃Al layer was predominant. Cracking at the wirebond interface was observed after 360 hours of aging as shown in Figure 25. The small peripheral crack was observed in between two phases of IMC. Unlike Cu and PCC wires, no cracking was observed at the interface of IMC-ball bond. The crack growth proceeded rapidly towards the center with increase in aging duration leading to eventual failure accompanied with bond lift after 1200 hours of thermal aging. In Ag wirebonds, even though cracks initiated at early stages of thermal aging, the resistance of the wirebond system did not degrade till much later in the accelerated test. Further, the interface cracks in the Ag-system were slow to propagate in comparison with the cracking in Cu and PCC wirebonds. A point of comparison, after 720 hours of aging the Ag-system, interface cracks covered 40-percent of the cross-section, but resistance increase was still in the neighborhood of 15-percent. The low increase in resistance even in the presence of significant cracking could be attributed to the higher electric conductivity of the Ag or very irregular crack growth in the out of plane direction.

Au Wirebond

Figure 26 shows change in resistance of Au-wirebonded packages at very high ambient temperatures. Red dashed line indicates failure threshold of 20-percent change in resistance. Failures were observed only after 360 hours of aging. Au-wirebonded packages failed fastest among all material candidates. Rate of change in resistance increased significantly after initial 120 hours of aging. Figure 27 shows change in the morphology of the bond-pad interface. Au wirebonds were found to have the thickest IMC in as bonded state, in comparison with Cu, PCC, and Ag wirebonds. Increase in thickness was observed as the aging duration increased. Voiding was observed in the IMC phases, along the periphery after 120 hours of aging. Extent of voiding increased with the aging time. Subsequent to 360 hours of aging, very thick but voided layer of IMC was observed.

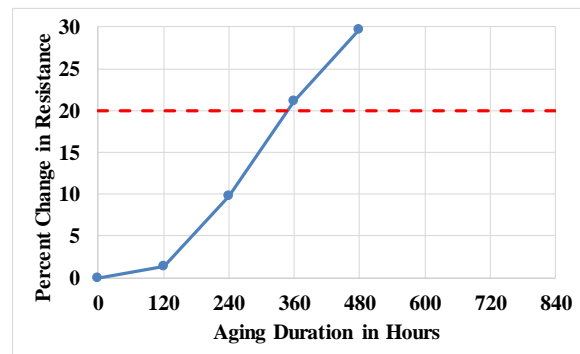


Figure 26. Increase in Resistance of Au-Al WB at 200°C aging temperature.

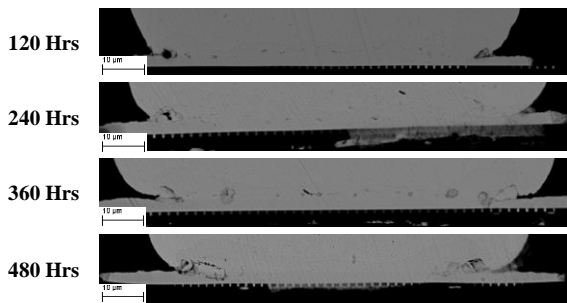


Figure 27. Growth of Au-Al IMC at bond-pad interface

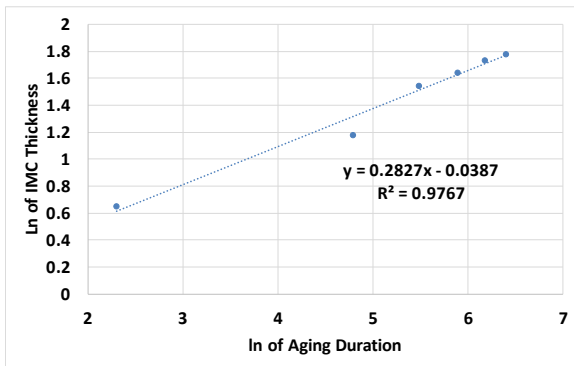


Figure 28. log-log plot of IMC thickness vs aging duration

Figure 28 shows log-log plot of increase of the IMC thickness due to thermal aging. Time exponent of the fit was found to be 0.28, which is least among all materials tested in the study, and shows high deviation from Fickian diffusion. Ideally, it is expected that the wirebond IMC will be dominated by Fickian diffusion, which was found to be true in case of Cu and PCC wires. However, in the case of Au wires, IMC, which has different physical properties, forms very thick layer at interface, and affects the diffusion rate. IMC phase transformation mechanisms may add to this effect, making it more pronounced. EDX scan was performed on the cross-sections is shown in Figure 29. Two phases were observed during the initial stages of aging shown in Figure 29(i), while only one phase was found at failure. Results of the EDX scan are shown in Table 6. Analysis revealed that in both Figure 29(i) and (ii), all observed phases were Au rich phases. The phase at point A in Figure 29(i) was Au_4Al and phase point B was Au_8Al_3 . Subsequent to failure, shown in Figure 29(ii), only Au_4Al phase was found which indicates that it is the terminal phase, and all other phases transform into Au_4Al . This is consistent with the results reported in [21], [22].

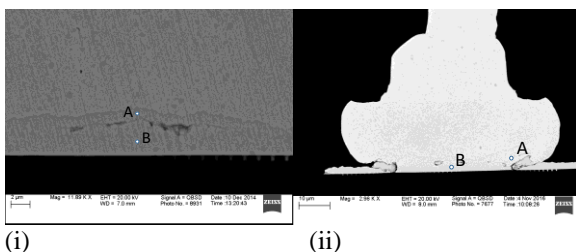


Figure 29. Phases in Au-Al wirebond system due to exposure to high temperature

Table 6. EDX analysis of IMC phases at point A, B

| Figure 29 | Element | Percent Atomic Content | |
|-----------|---------|------------------------|---------|
| | | Point A | Point B |
| (i) | Au | 80.38 | 69.40 |
| | Al | 19.62 | 30.60 |
| (ii) | Au | 82.26 | 81.53 |
| | Al | 17.74 | 18.47 |

In Au wirebonds, rapid phase transformation is observed with fast growing IMC layers. Due to very thick IMC, different phases of the IMC are supplied with Ag or Al atoms at different rates. The phase transformations at different rates along with higher diffusion rate of Au-Al system leads to Kirkendall voiding. Voiding becomes severe with the progression of aging, as shown in Figure 30. During the initial phases of aging, only minor voiding was observed. Voiding was focused at the interface of the two phases of the wirebond. Prolonged periods of aging resulted in the growth of voids and smaller voids merging to form larger voids. Location of such voids in between two IMC phases confirmed that different rates of the phase transformations were primary cause of the voiding. Au being chemically inert metal, does not show typical corrosion based degradation/cracking at the interface. In Au wires, voiding does not only reduce area available for current flow, but also weakens the Au-Al junction. Figure 31 shows change in shear strength of Au wirebonds over time. Initial observed strength of the bond was in the neighborhood of 52 grams. Au wires had higher initial shear strength due to well-developed and strong IMC that formed during the wirebonding process. Shear strength increased to 54-gram force after 120 hours of aging, and then dropped rapidly. Shear strength of the Au-wirebond degraded to 39 grams after 480 hours. Higher variance in the shear strengths was observed when wirebond started to degrade (after 120 hours of aging).

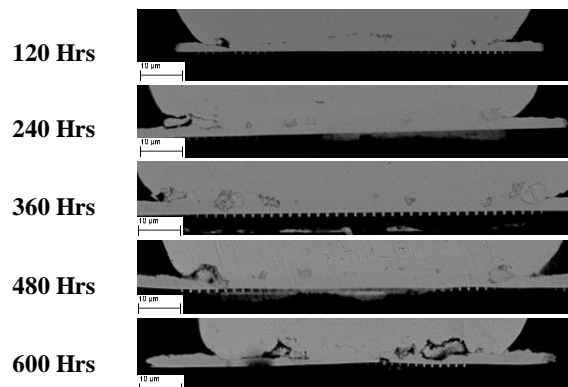


Figure 30. Voiding in Au-Al wirebonds

Figure 32 shows shear failure modes for Au wirebonds. In mode I (Figure 32a) type failure, bulk Au wire shears and the residue was found at the sheared interface. This is a desired mode of failure showing strong attachment of Au wire and Al pad. In mode II (Figure 32b) type failure, peripheral ring of residual IMC, along with clean lift at the

center of the ball bond was observed. The clean lift in the center was due to complete consumption of the Al pad. Even though Al pad has been consumed by Au along the periphery, the voided interface served as the weakest link and bond wire fractures along the voids, leaving a thick layer of IMC on the sheared surface. Similar type of failure was categorized as mode III when pad cracking was found beneath the ball bond (Figure 32c). Figure 33 shows the relative occurrence of each of the shear failure modes. In as bonded state, only mode I type failure was observed. However, after aging for only 120 hours, mode II type failure was found to dominate, and at the time of failure, only mode II type was observed. Transition from mode I to more II is very abrupt after 240 hours of aging. The change in the failure mode is accompanied with a rapid drop in shear strength in conjunction with significant voiding at the periphery of the ball bond as shown in Figure 30. Decreasing shear strength with mode II type failure, presence of large amount of voiding correlates well with the higher rate of increase in resistance, and eventual electrical failure.

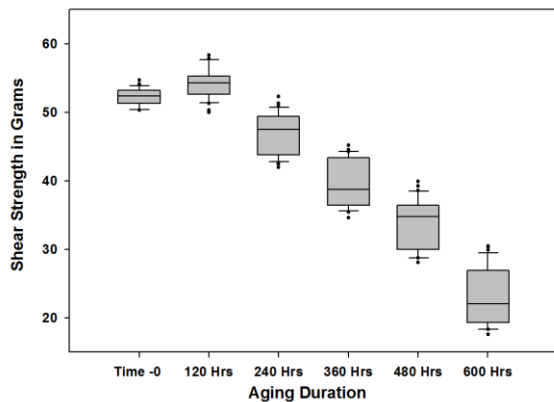


Figure 31. Change in shear strength of bond-pad interface as a function of time.

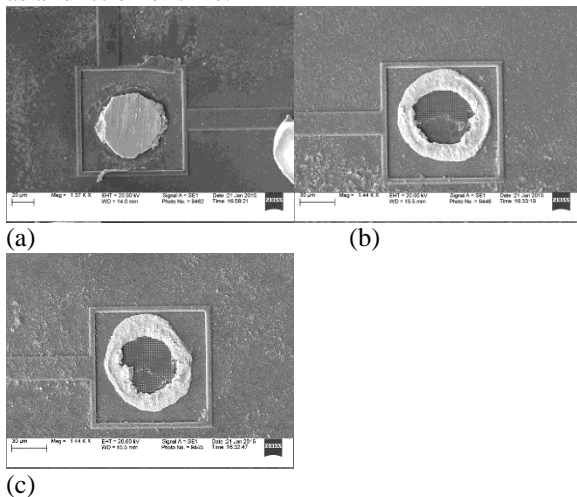


Figure 32. Shear failure modes (A) Mode I (B) Mode II (C) Mode III

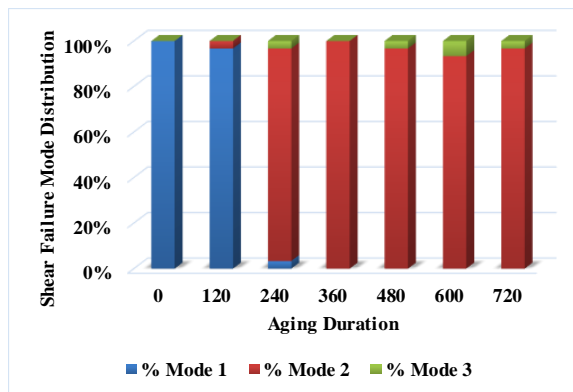


Figure 33. Evolution of shear failure modes

COMPARISON OF WIREBOND SYSTEMS

Figure 34 shows compiled resistance data for all four wirebond material candidates. Ag-wirebonded samples were found to be most reliable, exhibiting the longest time to 20-percent resistance increase and the lowest increase in resistance under HTSL, while the Au wirebonded packages were first ones to fail. In comparison with the gold wirebond system, Cu, Ag, and PCC wirebonds had slower rate of increase in resistance at the initial stages. Measurements indicate that the change in resistance of the wirebonds pairs correlates with the growth of different IMCs at the bond-pad interface, followed by degradation.

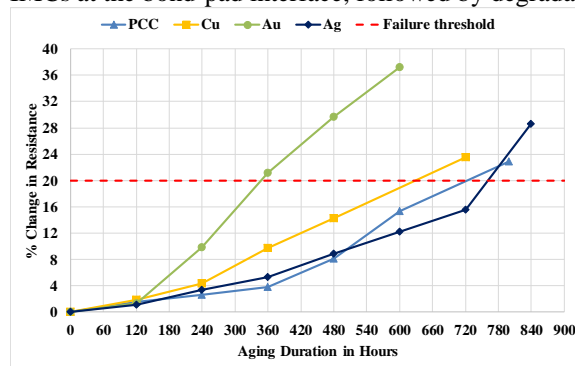


Figure 34. Change in resistance of wirebonds due to high temperature exposure

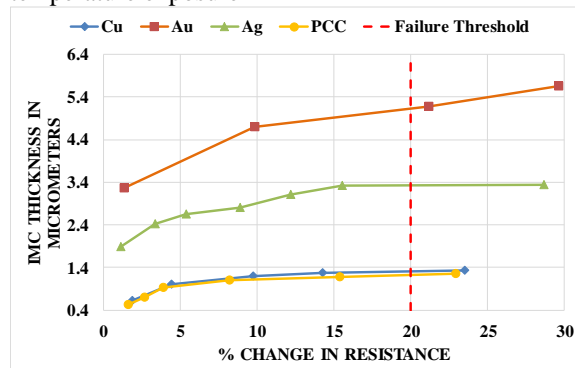


Figure 35. Change in resistance of the packages vs IMC growth.

The correlation between IMC thickness and resistance change is shown in Figure 35. For Cu and PCC wires, IMC thickness increases rapidly for first few data points. Once the resistance increase has reached 10-percent, the IMC

continues growth only at very slower pace. For Ag-wires, similar trend of change in the IMC growth rate with increase in resistance was observed with the change occurring in the neighborhood of 15-percent. Rapid resistance change observed before failure was due to the corrosion-based degradation of the IMC. For Au-wire, IMC continued to grow at a faster rate till failure. The Au-wirebond system degradation was triggered by growth of a thick IMC accompanied by Kirkendall voiding. Figure 36 shows log-log plot of IMC growth over time for all wirebond candidates. In as bonded state, Au had the highest IMC formation at the interface. Au-wirebond system had the highest growth rate amongst the systems in the study followed by Ag, Cu, and PCC wires. Presence of palladium at the bond pad interface was found to lower the IMC growth rate in comparison with bare Cu wires[1], [14], [16]. Similar behavior was observed in this study. Even though Ag had higher IMC thickness as well as growth rate than Cu, resistance increase for Ag wirebonds was slower than Cu wires. This can be attributed to higher resistivity of the Cu-Al IMC in comparison with Ag-Al IMCs. IMC growth in Cu and PCC wirebonds took place because of Fickian diffusion. Au and Ag wires did not follow this trend because of the thicker, faster, and voided IMC formation. Thicker IMCs may affect diffusion rates of the base-metals at the interfaces resulting in a slow-down of the IMC growth at during the final stages just prior to failure.

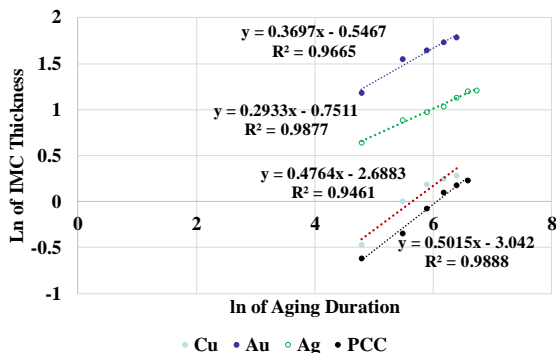


Figure 36. log-log plot of IMC growth over test time

Cu and PCC wirebonds had different shear failure modes than Au wirebonds. Au wirebonds had local detachment at the center and brittle fracture along the periphery (due to Kirkendall voiding) at the time of the failure. Cu and PCC wires showed peripheral cracking (corrosion based cracking) with much thinner IMCs and partial cracking at the center. Au-wirebonds exhibit excessive voiding at failure. Cu and PCC wirebonds damage progression was accompanied with corrosion based cracking along the periphery of the ball bond in the later stages of the aging. Highly localized random detachment of the ball bond from silicon was observed for Cu wirebonds. This is due to complete consumption of Al pad as shown earlier. For Ag wirebonds, even though crack was observed during the early stages of the aging, crack propagation was relatively slow and complete cracking was not observed even at failure.

SUMMARY AND CONCLUSIONS

Degradation of different wirebond material candidates including Ag, Au, Cu and PCC subjected to high-temperature thermal aging was presented in this paper. Performance of Au wirebond was considered as benchmark and compared with Cu, PCC, and Ag wirebonds bonded onto the Al-pad. Experiments were performed on molded 32-pin QFN daisy chained packages. Change in resistance of the wirebonds was observed using resistance spectroscopy technique. Acid based decapping process was used to remove the EMC and perform ball shear tests. Experimental measurements indicate that Cu and PCC wires had different modes of shear failure than Au wirebonds. Cross sectioning was used to study the bond interface. Au-wirebonds, which failed first had high IMC growth rate among all candidates. Presence of large voids reduced shear strength of the wire at much faster rate. Even though Ag wirebond had rapid IMC growth than Cu and PCC, it proved to be more reliable. This was because of high conductivity of the Ag IMC's and very slow crack propagation. Cu and PCC wires had very slow IMC growth rate. Upon failure, corrosion based microcracks and localized detachment was observed for both wires. Presence of Pd at the interface was found to lower the IMC growth and crack propagation rate, making it more reliable than Cu. Change in electric response of the wirebonds was then correlated with the IMC growth and cracking/voiding phenomenon. Changes in shear strength and shear failure modes were also correlated with the changes in the morphology of the bond-pad interface and increase in the resistance of the bond wires.

ACKNOWLEDGEMENTS

The project was sponsored by the Members of NSF-CAVE3 Research Center at Auburn University.

REFERENCES

- [1] Chauhan P., Choubey A., Zhong Z., Pecht M., "Copper Wire bonding" in *Copper Wire bonding*, Springer-Verlag Publisher, New York, USA. 2014
- [2] G. Hu, "Comparison of copper, silver and gold wire bonding on interconnect metallization," 13th International Conference on Electronic Packaging Technology and High Density Packaging (ICEPT-HDP), 2012, Guilin, 2012, pp. 529-533.
- [3] Inderjit Singh, J. Y. On and L. Levine, "Enhancing fine pitch, high I/O devices with copper ball bonding," Proceedings of Electronic Components and Technology, 2005, pp. 843-84.
- [4] Gan C., Ng E., Chan B., Classe F., Kwuanjai T., Hashim U., "Wearout reliability and intermetallic compound diffusion kinetics of Au and PdCu wires Used in Nanoscale Device Packaging", Journal of Nanomaterials, Vol 2013, Article ID 486373, pp1-9.
- [5] Goh C., Chong W., Lee T., Breach C., "Corrosion study and Intermetallics formation in Gold and Copper Wire Bonding in Microelectronics Packaging", Crystals Journal, Vol 3, 2013, pp 391-404.

- [6] Lall P., Deshpande S., Nguyen L., Murtuza M., "Microstructural Indicators for Prognostication of Copper Aluminum Wire bond reliability under high temperature storage and temperature humidity", IEEE Transactions on component, packaging and manufacturing technology, Vol 6, Issue 4, April 2016, pp 569-585.
- [7] K. Wieczorek-Ciurowa, K. Gamrat, and Z. Sawłowicz, "Characteristics of CuAl₂-Cu₉Al₄/Al₂O₃ nanocomposites synthesized by mechanical treatment," J. Thermal Anal. Calorimetry, vol. 80, no. 3, pp. 619-623, 2005.
- [8] Y. H. Tian, C. J. Hang, C. Q. Wang, G. Q. Ouyang, D. S. Yang, and J. P. Zhao, "Reliability and failure analysis of fine copper wire bonds encapsulated with commercial epoxy molding compound," Journal of Microelectronics Reliability., vol. 51, no. 1, pp. 157-165, 2011.
- [9] R. Rongen, G. M. O'Halloran, A. Mavinkurve, L. Goumans and M. L. Farrugia, "Lifetime prediction of Cu-Al wire bonded contacts for different mould compounds," 64th IEEE Electronic Components and Technology Conference (ECTC), Orlando, FL, 2014, pp. 411-418.
- [10] Peng Su, Seki H., Chen Ping; Zenbutsu, S.; Itoh, S.; Huang, L.; Liao, N.; Liu, B.; Chen, C.; Tai, W.; Tseng, A., "An evaluation of effects of molding compound properties on reliability of Cu wire components," 61st IEEE Electronic Components and Technology Conference (ECTC), 2011 pp.363-369.
- [11] Varughese M., Sheila C., Higgins L., Zhang Y. "Copper Wirebond Compatibility with Organic and Inorganic Ions Present in Mold Compounds", 46th International Symposium in Microelectronics, Sept 2013, Orlando Fl., pp 89-93.
- [12] P. Lall, S. Deshpande and L. Nguyen, "Principal Components Regression Model for Prediction of Acceleration Factors for Copper-Aluminum Wirebonds Subjected to Harsh Environments," 2016 IEEE ECTC Conference, Las Vegas, NV, 2016, pp. 637-647.
- [13] S. Kaimori, T. Nonaka and A. Mizoguchi, "The development of Cu bonding wire with oxidation-resistant metal coating," in IEEE Transactions on Advanced Packaging, vol. 29, no. 2, pp. 227-231, May 2006.
- [14] Lim A., Chang A., Lee C., Yauw O., Chylak B., Chen Z., "Palladium-coated Copper Wire Study for Ultra-Fine Pitch Wire Bonding", Transactions of Electro-Chemical Society, vol. -52, 2013, pp 717-730
- [15] Tang L., Ho H., Zhang Y., Lee Y., Lee C., "Investigation of Palladium Distribution on the Free Air Ball of Pd-coated Cu wire," Proceedings of 12th Electronics Packaging Technology Conference (EPTC), 2010, pp. 777-782.
- [16] Abe H., Kang D., etc. all, "Cu Wire and Pd-Cu Wire Package Reliability and Molding Compounds", Proceedings of IEEE ECTC Conference, 2012, pp 1117-1123.
- [17] Yoo K., Uhm C., Kwon T., Cho J., Moon J., "Reliability Study of Low Cost Alternative Ag Bonding Wire with Various Bond Pad Materials", Proceedings of 11th IEEE EPTC Conference, 2009, pp 851- 857.
- [18] Kai L., Hing L., Wu L., Chiang M., Jiang D., Huang C., Wang Y., "Silver Wire Bonding", 2012 IEEE 62nd Electronic Components and Technology Conference, San Diego, CA, 2012, pp. 1163-1168.
- [19] J. Xi et al., "Evaluation of Ag wire reliability on fine pitch wire bonding," IEEE 65th Electronic Components and Technology Conference (ECTC), San Diego, CA, 2015, pp. 1392-1395.
- [20] Lall P., Deshpande S., Nguyen L., "Fuming Acid Based Decapsulation Process for Copper-Aluminum Wirebond System Molded with Different EMC's", Proceedings of 2015 ASME InterPACKICNMM Conference, July 6-9, 2015 San Francisco USA.
- [21] Xu H., Liu C., Silberschmidt V., Chen Z., "Growth of intermetallic compounds in thermosonic copper wire bonding on Al metallization", Journal of Electronic Materials, vol 39, pp124-131, 2010.
- [22] H. Xu, C. Liu, V.V. Silberschmidt, S.S. Pramana, T.J. White, Z. Chen, V.L. Acoff, Behavior of aluminum oxide, intermetallics and voids in Cu-Al wire bonds, Acta Materialia, Volume 59, Issue 14, August 2011, Pages 5661-5673
- [23] Maeda M. and H. Seki, "Study of EMC for Cu bonding wire application," Electronic Packaging Technology (ICEPT), 2013 14th International Conference on, Dalian, 2013, pp. 393-395.
- [24] F. W. Wulff, C. D. Breach, D. Stephan, Saraswati and K. J. Dittmer, "Characterization of intermetallic growth in copper and gold ball bonds on aluminum metallization," Proceedings of 6th Electronics Packaging Technology Conference, 2004. EPTC, pp. 348-353.
- [25] I. Qin et al., "Wire bonding of Cu and Pd coated Cu wire: Bond ability, reliability, and IMC formation," 2011 IEEE 61st Electronic Components and Technology Conference (ECTC), Lake Buena Vista, FL, 2011, pp. 1489-1495.
- [26] Johnny Yeung PH, Hui Xu, Effie Chew, "Effect of palladium on copper aluminide intermetallic growth in palladium copper bonding wire", 13th International Conference on Electronic Packaging Technology and High Density Packaging (ICEPT-HDP) 2012, pp. 346-351, 2012.
- [27] Peng Su, Hidetoshi Seki, Chen Ping, Shingo Itoh, Louie Huang, Nicholas Liao, Bill Liu, Curtis Chen, Winnie Tai, Andy Tseng, "Effects of reliability testing methods on microstructure and strength at the Cu wire-Al pad interface", 2013 IEEE 63rd Electronic Components and Technology Conference (ECTC), pp. 179-185, 2013, ISSN 0569-5503.
- [28] C. H. Cheng, H. L. Hsiao, S. I. Chu, Y. Y. Shieh, C. Y. Sun and C. Peng, "Low cost silver alloy wire bonding with excellent reliability performance," 2013 IEEE 63rd Electronic Components and Technology Conference, Las Vegas, NV, 2013, pp. 1569-157.

- [29] Y. C. Jang et al., "Study of intermetallic compound growth and failure mechanisms in long term reliability of silver bonding wire," Electronics Packaging Technology Conference (EPTC), 2014 IEEE 16th, Singapore, 2014, pp. 704-708.